J. Membrane Biol. 57, 103–118 (1980)

The Journal of
Membrane Biology

Ion Conductance and Ion Selectivity of Potassium Channels in Snail Neurones*

H. Reuter** and C.F. Stevens
Department of Physiology, Yale University School of Medicine, New Haven, Connecticut 06510

Summary. Delayed potassium channels were studied in internally perfused neurone somata from land snails. Relaxation and fluctuation analysis of this class of ion channels revealed Hodgkin-Huxley type K channels with an average single channel conductance (γ_K) of 2.40 ± 0.15 pS. The conductance of open channels is independent of voltage and virtually all K channels seem to be open at maximum K conductance (g_K) of the membrane. Voltage dependent time constants of activation of g_K, calculated from K current relaxation and from cut-off frequencies of power spectra, are very similar indicating dominant first-order kinetics. Ion selectivity of K channels was studied by ion substitution in the external medium and exhibited the following sequence: $Tl^+ > K^+ > Rb^+ > Cs^+ > NH_4^+ > Li^+ > Na^+$. The sequence of the alkali cations does not conform to any of the sequences predicted by Eisenman's theory. However, the data are well accommodated by a new theory assuming a single rate-limiting barrier that governs ion movement through the channel.

Molluscan neurones show a complicated pattern of outward currents when studied under voltage-clamp conditions. At least three time- and voltage-dependent outward currents, predominantly carried by K^+ ions, have been identified: 1) A transient outward current that activates and inactivates at negative potentials ("A" current, Connor & Stevens, 1971*b*; Neher, 1971); 2) A delayed outward current that behaves kinetically like K currents in squid axon and node of *Ranvier* (Connor & Stevens, 1971*a*; Meech & Standen, 1975; Adams & Gage, 1979); 3) A Ca^{2+}-activated K outward current that superimposes the delayed outward current (Meech & Standen, 1975; Heyer & Lux, 1976). This probably also is the current identified by Partridge and Stevens (1976) as responsible for spike frequency adaptation.

The various components of outward current can be separated either kinetically or by pharmacological means (Meech & Standen, 1975; Heyer & Lux, 1976; Thompson, 1977).

Our goal in this study has been to characterize one class of K channels in greater detail, those carrying the delayed outward current, and particularly to define the ionic selectivity of these channels. The investigations of delayed K channels reported here used unidentified neurone somata from land snails (*Helix roseneri*). The results show that single-channel conductance of this class of K channels is independent of voltage and virtually all channels open at peak K conductance. The alkali metal cation selectivity of these channels cannot be simply explained by equilibrium ion exchange selectivity (Eisenman, 1962; for reviews *see* Diamond & Wright, 1969; Hille, 1977). However, our experimental results are well accommodated by a new selectivity theory described below.

Materials and Methods

Preparation

Circumoesophageal rings of ganglia were quickly dissected from land snails (*Helix roseneri*, Connecticut Valley, Biological Supply Company, Southhampton, Mass.). The suboesophageal ganglia were pinned dorsal side upward to a layer of Sylgard (Dow Corning Corporation) coating an aluminum chamber. The preparations were exposed for about 15 min to an isotonic solution (external solution 1, Table 1) containing 0.1% trypsin. This facilitated the subsequent removal of the thick and thin connective tissue sheets covering the nerve cells, and, later on, the isolation of single neurone somata. In control experiments without the addition of trypsin we could exclude any effect of the enzyme

* *This paper is dedicated to the memory of Walther Wilbrandt.*

** *Permanent address:* Department of Pharmacology, University of Bern, Friedbuhlstraße 49, 3010 Bern, Switzerland.

0022-2631/80/0057-0103 $03.20

Table 1. Ionic compositions of internal and external perfusion solutions (in mM/liter)

	NaCl	KCl	$CaCl_2$	$MgCl_2$	K-aspartate	EGTA	Hepes	pH
Internal:								
1	–	5	–	–	110	3	1	7.1
2	3	2	–	–	110	3	1	7.1
External:								
1[a]	100	4	2	15	–	–	10	7.3
2[b]	–	110	1	15	–	–	10	7.3

[a] Normal. [b] (KCl).

treatment on the membrane currents investigated in these experiments. During the experiments the solutions in the bathing chamber were cooled to 12–16 °C by means of a Peltier device (Cambion, Cambridge, Mass.).

Solutions

The compositions of the salt solutions used for internal and external perfusion of the neurones are listed in Table 1. When we studied the ion selectivity of potassium channels we replaced KCl in external solution 2 (Table 1) by osmotically equivalent amounts of the following salts: LiCl, NaCl, RbCl, CsCl, $CaCl_2$, $MgCl_2$, $BaCl_2$, $SrCl_2$, NH_4Cl, hydroxylamine · HCl (pH 6, *cf.* Hille, 1973), a mixture of hydrazine · 2 HCl and hydrazine, methylamine · HCl, guanidinium · HCl. Since TlCl is only poorly soluble in water, an isotonic Tl-acetate solution was compared with a corresponding K-acetate solution. One mM KCl was added to these solutions in order to stabilize the bath electrode potentials.

Experimental Set-up

We followed the original suggestion by Kostyuk, Krishtal and Pidoplichko (1975) and Kostyuk and Krishtal (1977) for external and internal perfusion of single, isolated snail neurone somata. Our design of the perfusion pipette (Fig. 1) is a modification of that recently described by Lee, Akaike and Brown (1978).

The tip of the pipette (Fig. 1) was drawn from glass tubes (outer diameter about 1.6 mm, inner diameter about 1.2 mm) with a conventional micro-electrode puller. The tip was broken and fire-polished (inner diameter 10–22 μm) by means of a microforge (Stoelting, Chicago, Ill.). The glass tip was glued with beeswax onto the plastic tip (volume 1.8 ml) of an Eppendorf pipette. Inserted into the pipette were inlet and outlet polyethylene tubes for internal perfusion, an Ag/AgCl voltage electrode, and a glass tube (outer diameter 2 mm) which was covered with rubber membranes at both ends. The glass tube was filled with vaseline. It served as guidance for a platinum-iridium wire (diameter 0.1 mm) melted into a thin polyethylene tube. The plastic-coated platinum wire was pushed through tightly fitting holes in the rubber membranes and through the vaseline-filled core of the glass tube. This design permitted movement of the platinum wire through an air-tight guidance. The uncoated tip of the platinum wire was electrolytically sharpened to 2–5 μm in a solution of 50% NaCN and 30% NaOH by applying a.c. between the wire and a carbon rod (Wolbarsht, MacNichol & Wagner, 1960). The sharpened tip of the platinum wire could be inserted into the cell body and served as current electrode (*see* Fig. 1). The top of the plastic pipette was closed by melting beeswax around inlet and outlet tubings and electrodes.

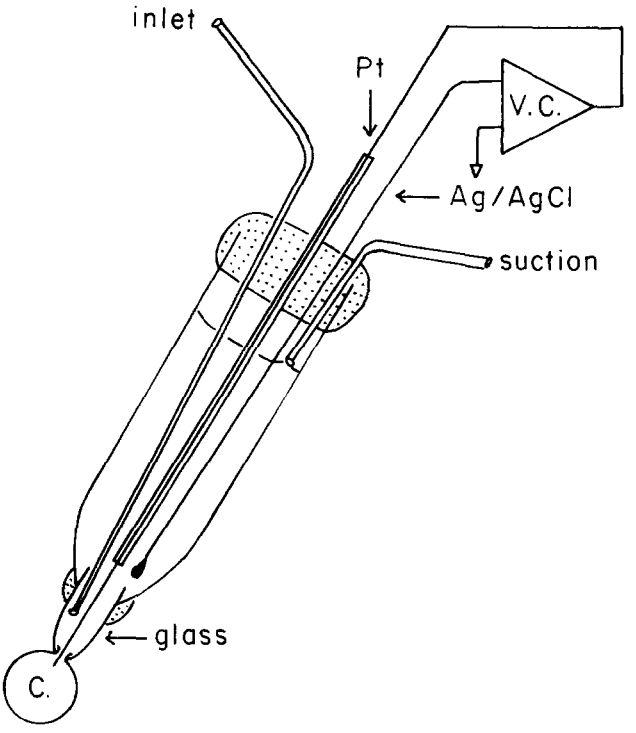

Fig. 1. Schematic representation (not drawn to scale) of the suction pipette, voltage-clamp system used in this study. Stippled areas: beeswax; *c*: cell body; *Pt*: platinum-iridium wire pushed through vaseline-filled glass tube (=current-passing electrode; Ag/AgCl wire (=Voltage electrode); *V.C.*: Voltage clamp amplifier. For extensive description *see* text

The glass tip of the pipette was thinly coated with a glue prepared from 60% liquid paraffin oil and 40% Parafilm (Kostyuk & Krishtal, 1977). The glue was evenly distributed over the rim of the glass tip by passing a hot air-stream over it. This was an essential procedure for obtaining high seal resistances between glass tip and cell body and had to be repeated before each experiment.

Voltage electrode (Ag/AgCl wire) and current electrode (platinum-iridium wire) were connected to a standard voltage clamp amplifier (Fig. 1). Membrane potential was measured between the Ag/AgCl wire in the pipette and another Ag/AgCl pellet placed in the bathing solution. Current was measured differentially relative to virtual ground, with the possibility to partially compensate for series resistance. Constant current was injected into the cell through a 10^8 Ω resistor. A programmable stimulator (Sigworth, 1979) delivered constant current pulses or command pulses for voltage clamp. Pulse pattern and pulse sequence were controlled by a computer (PDP 11/34, Digital Equipment Corp., Marlboro, Mass.).

Experimental Procedure

After removal of the connective tissue sheaths surrounding the suboesophageal ganglia, the tissue was extensively washed with normal bathing solution (external solution 1, Table 1). Single cells were easily seen under a stereomicroscope. All experiments were

performed on unidentified cells from the left or right parietal ganglia. Cell bodies with diameters between 80 and 150 μm were selected for most of our experiments. The suction pipette shown in Fig. 1 was mounted on a Leitz micromanipulator and filled with internal solution 1 (Table 1). Negative pressure was applied by means of a glass syringe connected to the outlet tube (Fig. 1) then the pipette was advanced toward a cell soma. After aspiration of a cell body to the tip of the suction pipette, the soma was disconnected from its axon by slow motion of the micromanipulator. The disruption of the axon occurred usually within 500 μm distal to the soma. The isolated cell on the tip of the suction pipette was transferred through a fluid-filled groove into a neighboring chamber, where bathing fluids could be rapidly changed.

The quality of the seal between pipette tip and aspirated cell soma was judged by the increment in the voltage displacements resulting from hyperpolarizing constant current pulses (5 nA). The pipette resistance was about 100 KΩ. When cells were aspirated, the resistance initially increased up to 100 MΩ. After disruption of the cell membrane in the opening of the tip by suction and/or penetration of the platinum electrode, the resistance decreased again, and the voltage traces showed single exponential time courses with time constants between 10 and 50 msec. In normal saline (external solution 1, Table 1) the average input resistance was 12.7 ± 1.6 MΩ (mean ± SE). This is very similar to the input resistance measured in these cells with two intracellular microelectrodes (12.1 ± 1.9 MΩ; Meves, 1968). The input resistance dropped to 5.4 ± 1.0 MΩ when normal saline was replaced by isotonic KCl solution (external solution 2). Series resistance was estimated as 160 ± 20.5 KΩ from instantaneous voltage jumps in response to a current step.

Some evidence for the efficiency of internal perfusion of the cell with a similar system has been presented by Lee et al. (1978). Further evidence will be presented in the *Results*.

Leak currents and capacity transients were measured at hyperpolarizing clamp steps to −140 mV and linearly subtracted from currents at more positive potentials. Linear leak subtraction was justified from currents measured after blockage of time-dependent conductances by TTX, cadmium and TEA. Under these conditions the current-voltage relation was linear over a wide range of potentials.

The cells remained in reasonably stable condition for at least one hour after isolation. During this time $\bar{g}_K$ decreased on the average by 11% and leakage conductance remained constant. Inward currents seem to be more sensitive since they usually became smaller and often disappeared within 20 minutes after starting the internal perfusion.

Reversal Potential Determination

The reversal potential V_o of the delayed outward current was determined in various external cation solutions (*see* Results), while the internal solution (solution 1 in Table 1) was kept constant. V_o was obtained from instantaneous current-voltage relationships (*cf.* Hille, 1973). After the delayed outward current was first activated by a constant voltage step of 32 msec duration, the membrane potential was rapidly changed to another value where the current relaxed to a new steady state (tail currents, *see* Fig. 3). The second voltage step was taken to different levels. The membrane potential at which no relaxing tail current could be detected was taken as V_o. In order to determine V_o as accurately as possible under various external conditions, instantaneous current voltage relations were repeated several times in the same experiment with two alternating isotonic salt solutions (e.g., KCl and NaCl, or NaCl and LiCl, etc.). In useful experiments, V_o was usually reproducible within 2–3 mV; for a given solution, average values were calculated from the multiple determinations of reversal potential.

A possible artifact in the determination of V_o could result from K^+ accumulation just outside the cell membrane (Hille, 1973; Neher & Lux, 1973; Heyer & Lux, 1976). K efflux during the first voltage step could cause such K^+ accumulation. With nonpermeant, organic or divalent cations in the external solution (i.e., in the nominal absence of external K^+) small inward currents could occasionally be observed which reversed at potentials negative to −100 mV (*see* Fig. 10). If external K^+ accumulation at the outer membrane surface is responsible for this poorly reproducible V_o, it was at most 1–2 mM as calculated from the Nernst equation (assuming that the internal K^+ concentration remained constant with internal perfusion). However, even for the most poorly permeant alkali cation (Na^+), the reversal potential was at least 30 mV more positive than that expected from K^+ accumulation.

Fluctuation Analysis

The method used for recording and analyzing noise from delayed potassium channels was similar to that described by Begenisich and Stevens (1975; *see also* Neher & Stevens, 1977). All noise experiments were performed with identical intracellular and extracellular K^+ concentrations (internal solution 1, external solution 2, Table 1). Membrane potential was held at −40 mV (holding potential). Before and after sampling noise at various membrane potentials, the activation range of the delayed K^+ conductance (i.e., $g_K(\infty)/\bar{g}_K$) was explored and the reversal potential V_o was determined. Potassium current (i_K) noise could be measured reliably in the potential range between +30 and +110 mV, corresponding to a g_K activation range between 0.5 and 0.95.

Noise was sampled during voltage clamp steps of 256 or 512 msec. Clamp pulses were applied every 3 sec. Inactivation of g_K during such clamps was usually less than 10%. Possible use-dependent effects on i_K were avoided by clamping several times to the same potential before actual current samples were taken. Mean currents were recorded at a gain of 100, while current noise was further amplified by a factor of 200. High gain current traces were filtered through a 1000 Hz active low pass filter and a 4 Hz gated high pass filter. The current traces were fed into a digital computer (PDP 11/34) which sampled the currents at a rate of 1024 Hz. Spectral densities over the frequency range between 4 Hz and 512 Hz were analyzed by the fast Fourier transform routine (Anderson & Stevens, 1973; Neher & Stevens, 1977). The average spectra of 30–60 current traces produced a final power spectrum. This final spectrum was integrated to yield the variance (σ^2) of the current fluctuations. In addition to noise spectra obtained in the activation range of the potassium conductance at positive membrane potentials, we also measured current noise at corresponding negative membrane potentials. These control spectra, which contained components of instrumental noise, thermal noise, leakage noise, etc., were subtracted from the spectra at corresponding positive potentials where g_K was activated. The subtracted spectra were sometimes smoothed according to the weighting (hanning)

$$\bar{X}_n = (X_{n-1} + 2X_n + X_{n+1})/4$$

where X_n is the spectral density for the n^{th} frequency band, and $\bar{X}_n$ is the corresponding smoothed value.

Results

General Properties of Delayed Potassium Current

Fig. 2 shows typical current records obtained from single snail neurones in normal external solution (*a*)

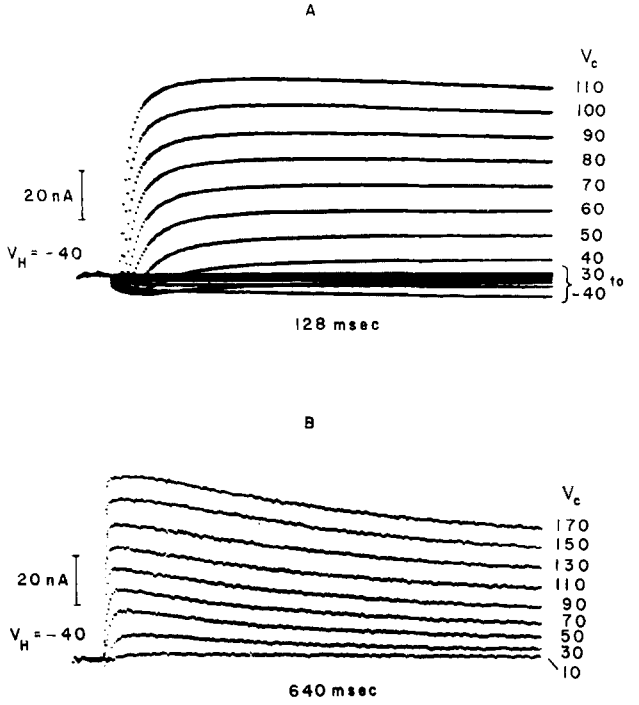

Fig. 2. Current traces measured from two snail neurones at different sample lengths of 128 msec, (*A*) and 640 msec (*B*). Currents in (*A*) were measured in normal external solution, those in (*B*) in KCl-solution; internal solution 1 in both experiments (Table 1). Holding potentials $V_H - 40$ mV; clamp potentials V_C indicated on right-hand side of current records. Cells SK-24 and SK-48; $T = 16$ °C

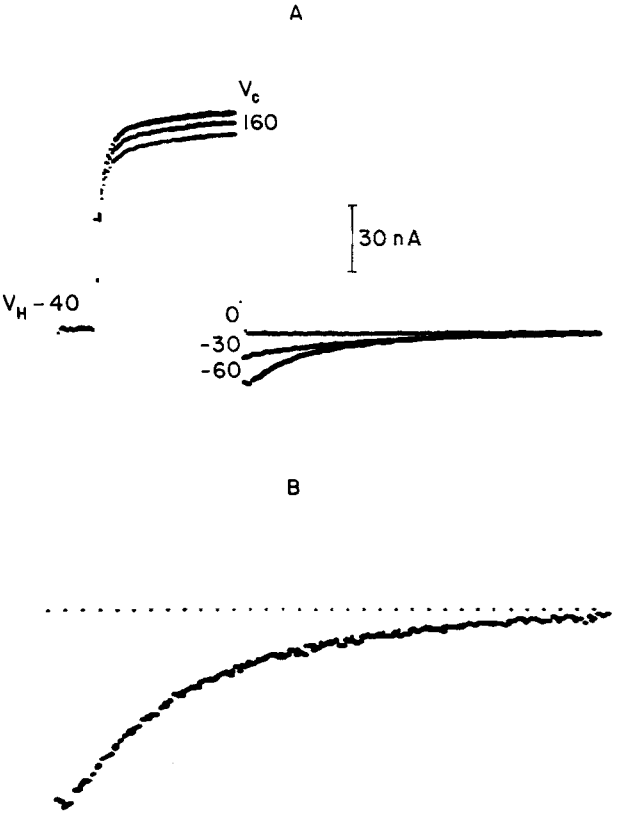

Fig. 3. Current traces recorded from snail neurone during double-step voltage clamps. Cell bathed in KCl solution, internal solution 1 (Table 1). The first step (32 msec) clamped the membrane potential to +160 mV (the decrease in current is due to "use dependence"; *see text*), the second steps to 0, −30 or −60 mV (*A*); the reversal potential V_o is at 0 mV. The current trace at −60 mV is enlarged in (*B*) and fitted by an exponential with a time constant of 16 msec. Cell SK-14, $T = 16$ °C

or KCl solution (*b*). The holding potential (V_H) was set to −40 mV, in order to inactivate the rapid outward "A" current (Connor & Stevens, 1971*b*; Neher, 1971; Thompson, 1977). Leak currents and capacity transients were linearly subtracted. Voltage clamp command pulses have been applied in 10 mV (Fig. 2*a*) or 20 mV (Fig. 2*b*) steps. Fig. 2*a* shows inward currents in the voltage range −30 to +80 mV and delayed outward currents at potentials positive to −10 mV. Only outward currents which inactivate during long clamp steps are seen in Fig. 2*b*. However, inactivation was not always as prominent as in this example, particularly at temperatures below 16 °C.

Fig. 3 depicts current records obtained with a pulse pattern different from that in Fig. 2. This cell was bathed in isotonic KCl solution. A first clamp step of 32 msec duration depolarized the membrane from a holding potential of −40 mV to +160 mV which fully activated the delayed outward current. A second step repolarized the membrane to −60, −30 or 0 mV. The current trace at the second step was flat at the reversal potential ($V_o = 0$ mV), while inward current tails were seen at negative potentials and outward current tails (not shown) at positive potentials. V_o at 0 mV was expected with identical internal and external K^+ concentrations. The inward current tail at −60 mV is shown at a higher gain in Fig. 3*b*. It could be fitted by a single exponential. Maximal tail currents at the beginning of the second clamp steps were plotted against the voltage at these steps (instantaneous current-voltage relationships, Figs. 4*b* and 5*b*). The conditioning outward current at the first step decreased somewhat during consecutive depolarizations. This "use-dependence" was corrected for and taken into account for plots of instantaneous current-voltage relationships. Current patterns similar to those shown in Figs. 2 and 3 have been described before for a variety of molluscan neurone somata (Connor & Stevens, 1971*a*; Neher, 1971; Kostyuk, Krishtal & Doroshenko, 1975; Thompson, 1977; Meech, 1978).

There appears to be one important difference

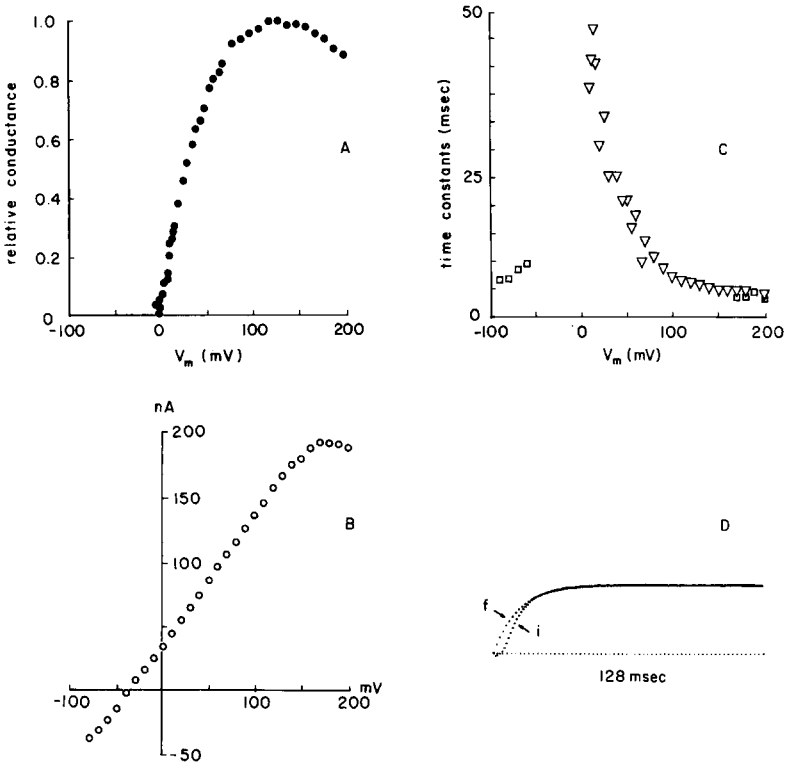

Fig. 4. Kinetic parameters of delayed K conductance obtained from a snail neurone perfused with internal solution 2, and bathed in normal external solution (Table 1). (*A*) Relative steady-state K conductance ($g_K(\infty)/g_K$) plotted as function of membrane potential V_m. (*B*) Instantaneous current-voltage relation; $V_o = -37$ mV. (*C*) Time constants of K current activation plotted against V_m. Time constants were estimated either by fitting the upper part of activating K current traces with exponentials (▽) as shown in (*D*) or from deactivating currents. (□; *see* Fig. 3*B*). The current trace (*i*) in (*D*) was measured during a clamp step to +65 mV and fitted by an exponential (*f*) with a time constant of 11.5 msec. Cell SK-6, $T = 14.5$ °C

between our outward current traces and those reported by others. Our outward currents did not show a secondary slower creep, and the final relaxation could be fitted by an exponential (Fig. 4*d*). A nonexponential creep of outward currents, however, has been reported by Meench and Standen (1975), Thompson (1977) and others. Correspondingly, these authors found a nonexponential decay of tail currents. The secondary component of outward current has been attributed to a Ca-activated K conductance which could be blocked either by injection of EGTA into the neurone (*see* Meech, 1978) or by the addition of cobalt to the external solution which inhibits Ca inward current (Meech & Standen, 1975; Thompson, 1977). Our internal perfusion solution always contained 3 mM EGTA (Table 1) which was apparently effective in eliminating the Ca-activated K current, as judged from the exponential time course of our outward and tail currents. Furthermore, N-shaped current-voltage relationships at positive potentials resulting from Ca-activated K current (Meech & Standen, 1975; Thompson, 1977) were not seen in our experiments (Figs. 4 and 5; *see also* Meech, 1978). Therefore, we were left with only one outward current component, the delayed K outward current present in many nerves and muscles (for review *see* Armstrong, 1975). This outward current was not affected by cadmium or high magnesium in the external solution which inhibit inward Ca current.

Fig. 4 shows plots of relative conductances ($g_K(\infty)/\bar{g}_K$; Fig. 4*a*), of instantaneous tail currents (Fig. 4*b*), and of time constants (Fig. 4*c*) of the delayed potassium current. The data were obtained from a cell bathed in NaCl-containing, normal external solution, and perfused with internal solution 2 (Table 1) which contained 3 mM NaCl. V_o was −37 mV. The limiting conductance $\bar{g}_K$ was 0.91 μS while steady-state conductance $g_K(\infty)$ at each membrane potential (V_m) was calculated from steady-state outward current (*cf.* Fig. 2*a*) divided by the driving force ($V_m - V_o$). The instantaneous current-voltage relationship (Fig. 4*b*) was linear over the voltage range −50 to +150 mV. However, at potentials positive to +150 mV the cell membrane rectified, i.e., the conductance decreased. This is most likely due to blockage of K channels by outward moving Na ions, since rectification occurred positive to the Na equilibrium potential (+91 mV). This assumption is supported by two other findings: (1) Rectification at positive potentials was never seen in the absence of internal and external Na^+ (Fig. 5), and (2) Na ions moving through the K channels in the inward direction also caused rectification (Fig. 9, Table 4). Block of K channels by Na ions in squid giant axons has been described by Bezanilla and Armstrong (1972).

The delay in onset of outward currents at any voltage step was variable. It could be quite prominent as in Fig. 4*d*, but it became quite short or

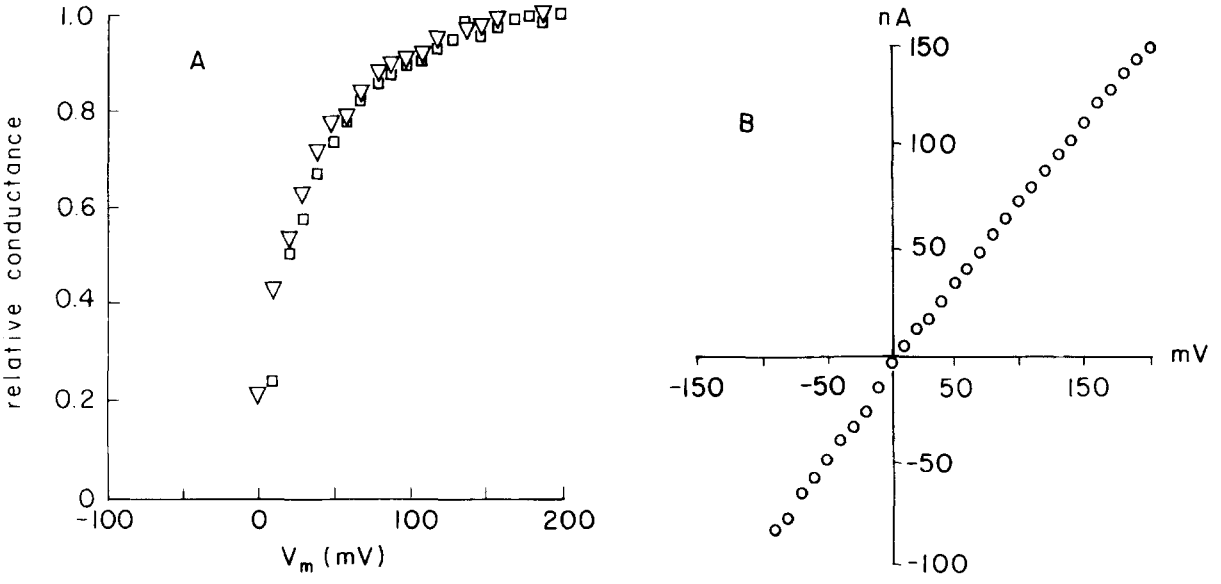

Fig. 5. (*A*) Relative K conductance ($g_K(\infty)/g_K$) and (*B*) instantaneous current-voltage relationship measured in a cell with identical internal and external K^+ concentrations (internal solution 1, external solution 2, Table 1). The two sets of data in (*A*) were obtained at the beginning (□) and end (▽) of a noise experiment; time interval 72 min. During this time $\bar{g}_K$ decreased from 0.89 to 0.76 μS. Cell SK-28, $T=16$ °C

virtually disappeared when cells began to deteriorate. We fitted the upper part of each current trace with an exponential and extracted the time constant from this fit (Fig. 4*d*).

At negative potentials we obtained the time constants from the exponential decay of tail currents (Fig. 3*b*). A plot of time constants *vs.* membrane potential is depicted in Fig. 4*b*.

Fluctuation Analysis of Potassium Channels

Potassium channel noise, that is current fluctuations presumably arising from gating of delayed K channels (Stevens, 1972), has been analyzed in different nerve preparations by various groups (squid axons: Conti, de Felice & Wanke, 1975; Fishman, Moore & Poussart, 1975; node of *Ranvier:* Siebenga, Meyer & Verveen, 1973; Begenisich & Stevens, 1975). However, the agreement between the results obtained from these groups is poor (Neher & Stevens, 1977). Therefore, we made another attempt at defining current noise associated with K channel gating in snail neurone somata. Specifically, we were interested in answering the following questions:

1) What is the conductance of a single K channel?
2) Do K channels have more than one open conductance state, and is the single-channel conductance voltage-dependent?
3) Does the step from closed to open state behave like a voltage-dependent first-order reaction?
4) What is the fraction of K channels open at peak K conductance ($\bar{g}_K$) of the membrane?
5) What is the density of K channels per surface area of membrane?

K channel noise has been measured successfully in nine cells bathed in isotonic K solutions (internal solution 1; external solution 2; Table 1). The activation of the K conductance can be expressed as fraction,

$$F = g_K(\infty)/\bar{g}_K$$

and the voltage range over which activation occurred was explored at the beginning and at the end of each experiment. Both measurements of the activation curve usually agreed within a few mV (Fig. 5*a*). V_o was determined by Instantaneous current-voltage relationships (Fig. 5*b*). During the course of these experiments $\bar{g}_K$ decreased from an average of 0.96 ± 0.18 (SE) to 0.85 ± 0.15 μS.

Current noise spectra were recorded at potentials within the activation range of g_K. Noise resulting from leakage currents at corresponding negative potentials (*see* Fig. 8) was subtracted. Corrected K current spectra are shown for two different potentials in Fig. 6. Within the accuracy of the measurements, the shapes of the spectra could be fitted by single time constant curves of the form (*see* Neher & Stevens, 1977)

$$S(f) = S(0)/(1 + (f/f_c)^2), \quad (1)$$

where $S(f)$ is the double-sided spectral density of

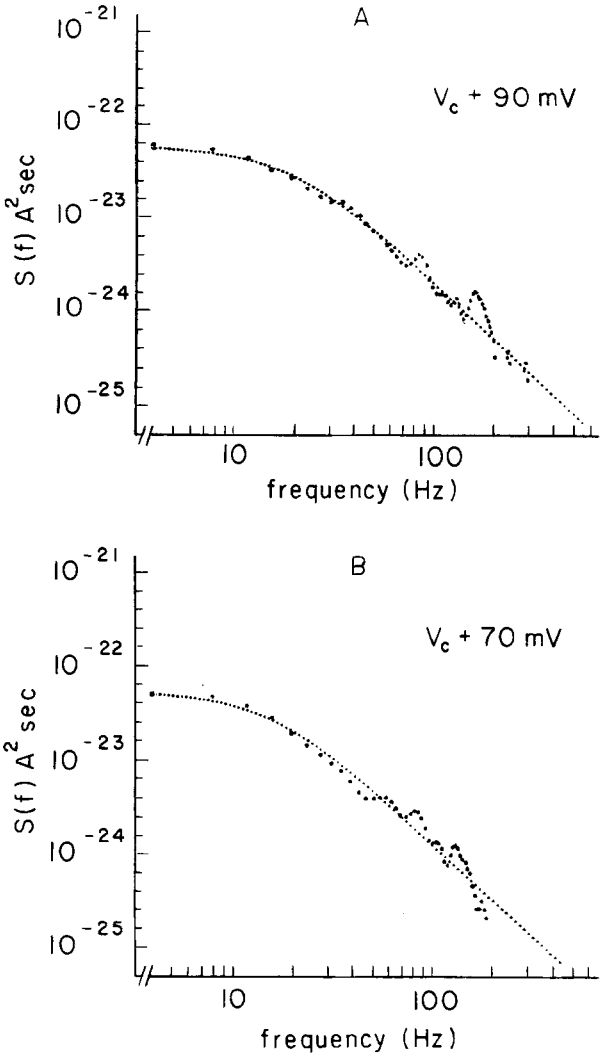

Fig. 6. Spectral densities $S(f)$ of K current fluctuations measured at +90 mV (*A*) and +70 mV (*B*). Spectra obtained from noise measurements at −90 and −70 mV have been subtracted. The corrected spectra were fitted by single Lorentzians with cut-off frequencies *fc* of 19.5 Hz (*A*) and 17.0 Hz (*B*). Spectral peaks at frequencies >60 Hz are power-line artifacts. Experimental spectra smoothed by hanning. Cell SK-43, $T=16.5$ °C

current, $S(0)$ is the zero frequency asymptote of the spectral density, f is the frequency of current fluctuations and f_c is the cutoff frequency. In three out of nine experiments the fits would have been slightly better by using two time constant spectral forms (*see also* Begenisich & Stevens, 1975). This, however, did not affect the estimate of the average single-channel conductance.

Integration of the spectra between 4 Hz (f_0) and 512 Hz (f_1) yields the variance σ^2 of current fluctuations,

$$\sigma^2 = \int_{f_0}^{f_1} S(f) \cdot df. \tag{2}$$

Table 2. Summary of K channel noise analysis

V_m (mV)	F	γ_K (pS)	τ (msec)	τ_K (msec)
30	0.58 ± 0.02	2.20 ± 0.47	13.3 ± 1.8	15.2 ± 1.3
50	0.77 ± 0.02	2.32 ± 0.35	11.7 ± 1.6	12.2 ± 1.5
70	0.86 ± 0.01	2.52 ± 0.38	10.3 ± 1.3	9.9 ± 1.2
90	0.90 ± 0.01	2.34 ± 0.36	8.6 ± 1.1	7.8 ± 1.2
110	0.93 ± 0.01	2.70 ± 0.34	6.8 ± 0.7	5.3 ± 0.5

V_m = membrane potential.
$F = g_K(\infty)/\bar{g}_K$.
γ_K = single-channel conductance.
τ = time constants calculated from cut-off frequencies of power spectra.
τ_K = time constants of K current activation.
Means ± SE.

Single-channel conductances (γ_K) were estimated from the variance by the equation

$$\gamma_K = \frac{\sigma^2}{\mu_K(V_m - V_o)(1-F)}, \tag{3}$$

where μ_K is the mean potassium current, V_m is membrane potential, V_o is the reversal potential, and F is the relative steady-state K conductance defined by $F = g_K(\infty)/\bar{g}_K$. From the spectra in Fig. 6 values for γ_K and f_c of 1.90 *pS* and 19.5 Hz (Fig. 6*a*, $V_m = 90$ mV) or 1.98 pS and 17 Hz (Fig. 6*b*, $V_m = 70$ mV) were obtained. In other words, γ_K is almost the same at both potentials, while the mean life-time of the channels ($\tau = 1/2\pi f_c$) decreases with further depolarization (8.2 and 9.4 msec, respectively). Table 2 summarizes the results obtained from nine experiments. In the g_K activation range (F between 0.58 and 0.93) the single-channel conductances are not statistically different, i.e., γ_K is independent of voltage. Moreover, the mean life-time of the channels calculated from the cut-off frequency (τ) is close to the relaxation time constant (τ_K) obtained from K current measurements (Fig. 4*c*, *d*). Both time constants show the same voltage dependences.

These results answer our first three questions:

1) The conductance of a K channel in the open state is 2.40 ± 0.15 pS (SE, $n=43$). This value of γ_K is slightly less than that reported by Begenisich and Stevens (1975) for node of *Ranvier* (4.09 ± 0.27 pS).

2) The conductance of open channels is independent of voltage, a conclusion also reached by Begenisich and Stevens (1975). This implies that K channels have probably only one open state.

3) The fit of the spectra by a single time constant form [Eq. (1)] implies first-order reactions between one or more closed states and one open state of the channels (Stevens, 1972; Anderson & Stevens, 1973).

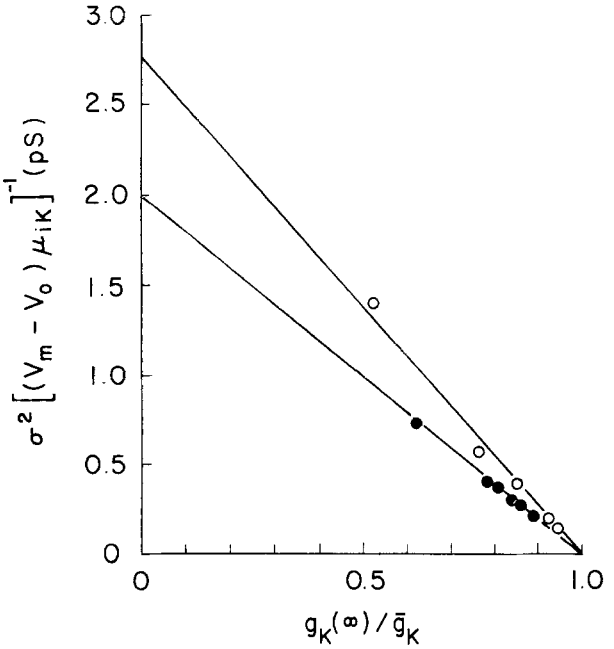

Fig. 7. Conductance obtained from K current noise [left-hand site of Eq. (5)] plotted as function of fractional K conductance, $F = g_K(\infty)/g_K$. Straight lines are least-square fits to the experimental data points from two cells (● SK-28; ○ SK-43). Further description in text

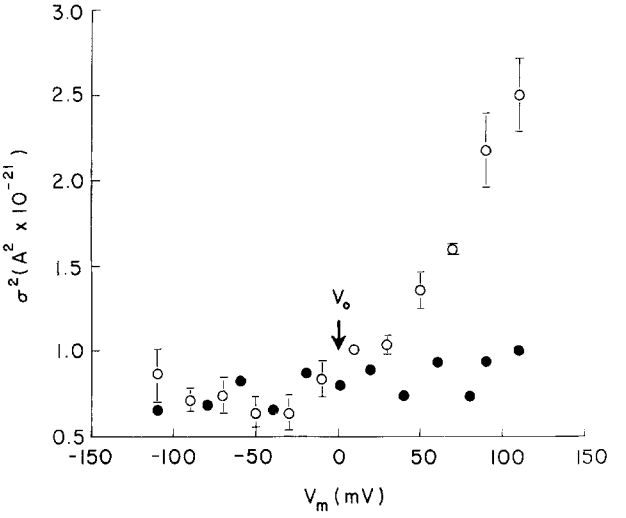

Fig. 8. Variance of current noise (ordinate) measured over a wide range of membrane potentials (abscissa). Results from four cells in isotonic KCl solution (means ±SE, open circles) and from one cell with 40 mM TEACl inside and outside (closed circles). V_o indicates average reversal potential of K current

The rate of these reactions is voltage dependent. The similarities between τ and τ_K in Table 2 support the assumption of dominant first-order kinetics.

Maximum K conductance $\bar{g}_K$ can be defined as

$$\bar{g}_K = \gamma_K \cdot N, \tag{4}$$

where N is the effective total number of open K channels. From combining Eqs. (3) and (4) and rearranging we obtain

$$\sigma^2/(\mu_K(V_m - V_o)) = \gamma_K - (\bar{g}_K/N)F. \tag{5}$$

This is a useful expression as shown in the plots of the results from two experiments in Fig. 7. The ordinate is the left-hand side of Eq. (5). To facilitate comparison of data from different experiments relative K conductance F has been plotted on the abscissa; the slope of the line fitted to the experimental data is $\bar{g}_K/N$. Extrapolation of the lines to the ordinate ($F=0$) yields values for γ_K [Eq. (5)] of 1.95 and 2.75 pS, respectively. The filled circles in Fig. 7 and the spectra in Fig. 6 are data from the same experiment. The agreement between the γ_K values obtained with both analyses (1.95 and 1.90–1.98 pS) is satisfactory. Good agreement between single-channel conductances evaluated with both methods was also obtained for the second experiment plotted in Fig. 7 (2.76 and 2.68 pS) as well as for other experiments.

The plots in Fig. 7 yield another important result. They provide an estimate of the fraction of channels that are open when K conductance reaches its peak. The variance is seen to vanish, that is, the ordinate is zero, for $F=1$. If the probability of a channel being open were less than one at $g_K(\infty)=\bar{g}_K$, the fitted lines should extrapolate to a point on the abscissa for which F exceeds unity. This observation suggests that virtually all K channels are open when K conductance is fully activated ($\bar{g}_K$), and provides an answer to our fourth question.

The density of K channels per μm^2 can be estimated from knowing $\bar{g}_K$, γ_K, and the membrane capacity C_m in each experiment. C_m could be obtained from capacity transients during small voltage-clamp steps. Assuming that a membrane capacity of 1 μF corresponds to a membrane area of 1 cm^2, we estimated a density of 7.2±1.6 K channels per μm^2.

What is the evidence that the current noise we have measured does indeed originate from fluctuations of *potassium channels*? The main evidence is presented in Fig. 8, where the total variance σ^2 of current noise is plotted against membrane potentials V_m at which membrane currents have been recorded. In this case σ^2 is the variance of current noise uncorrected for leakage current and measured at potentials between −110 and +110 mV. The results were obtained from five cells, four in the absence (open

circles) and one in the presence (closed circles) of tetraethylammonium ions (TEA). The variance is only slightly dependent on voltage over the range −110 to −30 mV. However, in the absence of TEA σ^2 rises steeply over the potential range −10 to +110 mV. This coincides exactly with the activation range of g_K (Figs. 4*a* and 5*a*). More importantly, with 40 mM TEA present in the external and internal solutions (KCl replaced by TEA Cl), there is neither an increase in σ^2 (Fig. 8) nor in g_K (not shown). TEA, however, is known to block potassium channels in snail neurones (Kostyuk et al., 1975; Meech & Standen, 1975; Heyer & Lux, 1976) as in other excitable membranes (Armstrong, 1975).

Ion Selectivity of Potassium Channels

Theory. Our goal here is to relate, at least in a provisional way, the reversal potential measurements presented in the next section to properties of the channel which reflect its molecular structure. To do so we must adopt a specific picture of ion permeation: we suppose that an ion moves through the channel by hopping over energy barriers separating one site from the next (*see* articles in Stevens and Tsien, 1979). After presenting the relation between reversal potential and barrier height, we develop a theory that links barrier height to physical properties of the channel (and water) structure.

We shall assume, for simplicity, that one position within the channel has the highest free energy, and that the barrier at this location is enough higher than its neighbors to be rate-limiting. In practice, this means we assume that selectivity occurs at a region whose free energy is several kilocalories per mole higher than that anywhere else within the pore. Further, we shall suppose that only single occupancy of energy minima near the rate-limiting barrier is possible, and that movement in this region of the channel must be single file.

As was first pointed out by Armstrong (Bezanilla & Armstrong, 1972) reversal potentials in certain simple situations reflect only barrier heights and not well depths (*see* Hille, 1975). For the general case with multiple arbitrary well and barrier energies, however, this simple situation does hold: reversal potential is a complicated function of all wells and barriers. If a channel has one barrier that is several kilocalories/mole higher than the others, a great simplification results because the occupancy of the channel is approximately that determined by equilibrium conditions. For a single rate-limiting barrier, then, it can be shown that reversal potential V_o is related (for monovalent cations) to the barrier height by the equation

$$V_o = \frac{RT}{F} \ln \frac{\sum m_{0k} \exp\left(\frac{-B_k}{RT}\right)}{\sum m_{1k} \exp\left(\frac{-B_k}{RT}\right)} \tag{6}$$

where m_{ok} and m_{1k} are the extra- and intracellular activities of the k^{th} ionic species, B_k is the height of the rate-limiting barrier for the k^{th} species, and R, T and F have their usual thermodynamic meanings.

We now establish the convention that potassium is a reference ion, and assign subscript $k=0$ for this species. Parenthetically, we note Eq. (6) may then be rewritten in the form of the familiar Goldman-Hodgkin-Katz equation (Goldman, 1943; Hodgkin & Katz, 1949)

$$V_o = \frac{RT}{F} \ln \frac{m_{oo} + \sum_{k \neq 0} m_{0k} P_k}{m_{1o} + \sum_{k \neq 0} m_{1k} P_k} \tag{7}$$

if the permeability ratio P_k is defined by

$$P_k = \exp^{\frac{-\Delta B_k}{RT}} \tag{8}$$

with $\Delta B_k = (B_k - B_o)$. Our standard conditions are to exclude all permeant ions other than potassium and to have inside and outside potassium activities equal; that is, $m_{oo} = m_{1o}$, and $m_{jk} = 0$ for all $k \neq 0$. In our experiments, we replaced the external potassium with the test ion. The only permeant species, then, were the internal potassium and the external test ion. We denote the reversal potential measured in this situation as V_k, which is thus related to ΔB_k by

$$\Delta B_k = -FV_k + RT \ln \left(\frac{m_{0k}}{m_{1k}}\right). \tag{9}$$

Eq. (9) relates, for our physical picture, barrier height to the observed reversal potential in the ion substitution experiments.

For ions such as the alkali metals, interactions with water and with their surroundings are almost entirely electrostatic (*see* Buckingham, 1957). This means that the only qualities of such an ion that enter into selectivity are those which influence the electric field around the ion; specifically, then, selectivity must depend upon ion radius and upon its valence. Because we shall concern ourselves only with monovalent cations, energy barrier height $B(X)$ will be considered to depend explicitly only on X, the reciprocal of the ion's radius. The dependence of barrier height on ion size can be represented as a

power series, where the function $B(X)$ has been expanded about X_o, the reciprocal radius of a reference ion (potassium in our case):

$$B(X)=B(X_o)+a_1(X-X_o)+a_2(X-X_o)^2 + a_3(X-X_o)^3+\ldots. \quad (10)$$

Buckingham's treatment (1957) of hydration energies indicates why reciprocal radius is the natural variable for this expansion. The number of terms that must be retained in this formal description depends on how selective the channel under study is. The acetylcholine-activated channel, for example, is known to be quite unselective and its selectivity barrier is well-described by only the first two terms in the expansion [Eq. (10)], the constant term and the one that depends linearly on reciprocal ion radius X (C.A. Lewis and C.F. Stevens, *unpublished observations*). Furthermore, the slightly more selective channels that require a quadratic term for their description, are those that give precisely the 11 Eisenman (1962) sequences (C.A. Lewis and C.F. Stevens, *unpublished observations*). The power series expression is useful, then, because it gives a more detailed and quantitative specification than do simple selectivity sequences, and it provides - through the number of terms required in the expansion - a characterization of the degree of a channel's selectivity.

The formal description of barrier height dependence on ion size, as embodied in Eq. (10), is useful in characterizing channel selectivity properties, but is potentially most valuable when the coefficients in the expansion (a_j) can be given a physical interpretation. The physical meaning for these coefficients can be expressed in terms of a theory based upon a general equation for the free energy of charges embedded in a dielectric medium.

The starting point of our development is an equation used by Born (1920) that gives the free energy of a charged metal sphere in a dielectric medium.

$$G(R)=\frac{1}{4\pi}\int_R^\infty dr\int_0^{2\pi} d\theta\int_0^\pi d\varphi\int_0^\varepsilon dq\, r^2\sin\varphi\,\frac{E(r,\varphi,\theta)}{r^2}. \quad (11)$$

$G(R)$ is the free energy of an ion of radius R, $E(r, \varphi, \theta)$ is the radial component of the electric field in the dielectric medium surrounding the ion, ε is the charge on the ion (we restrict consideration here to singly charged ions), and r, φ, θ are the length of the radius vector and angles for spherical coordinates. This equation is general and does not assume the dielectric medium is linear or isotropic or homogeneous. The electrostatic contribution to the selectivity energy barrier B is given by the difference in the free energy of an ion in solution (G_s) and the free energy at the "worst" point in the channel (G_c). B can therefore be expressed as

$$B(R)=\frac{1}{4\pi}\int_R^\infty dr\int_0^{2\pi} d\theta\int_0^\pi d\varphi\int_0^\varepsilon dq\, r^2\sin\varphi\,\frac{(E_c-E_s)}{r^2} \quad (12)$$

where E_c is the radial component of the electric field around the ion at the selectivity site, and E_s is the radial component of the electric field around the same ion in solution. This equation neglects any "chemical" interactions between the ion and its surroundings, and also assumes that the energy to create a cavity for each ionic species is the same. The radial component of an electric field E can be expressed as $E=D-4\pi P$, where D is the radial component of the dielectric displacement vector, and P is the radial component of the polarization vector, that is, the dipole moment per unit volume. The D field around an ion does not depend on the surrounding medium so the difference E_c-E_s is equal to the difference between the radial components of the corresponding polarization vectors P_c and P_s:

$$E_c-E_s=-4\pi(P_c-P_s). \quad (13)$$

Eqs. (12) and (13) can be written somewhat more compactly by averaging the polarization vectors over the surface of a sphere with radius R:

$$f=\int_0^{2\pi} d\theta\int_0^\pi d\varphi\, r^2\sin\varphi(P_c-P_s). \quad (14)$$

The quantity f gives the average density of dipoles on the surface of each spherical shell around the ion and depends on distance from the ion R. A straightforward calculation reveals that f should approach zero like $1/r$ as r becomes large. Eqs. (12), (13) and (14) permit the following simple expression for barrier height:

$$B(R)=\int_R^\infty dr\int_0^\varepsilon dq\,\frac{f}{r^2}. \quad (15)$$

This equation is further simplified by the change of variables $x=1/r$ and $X=1/R$:

$$B(X)=-\int_0^x dx\int_0^\varepsilon dq\, f(x,X,q). \quad (16)$$

Here, f has been indicated to depend explicitly on x, X and q.

Because the electric field around an ion depends on distance r from the ionic charge, the polarization vector does also. It is therefore clear why f, defined by Eq. (14), depends on this distance (expressed in Eq. (16) by its reciprocal, after the change in variable). The quantity f must also depend on q, the charge on

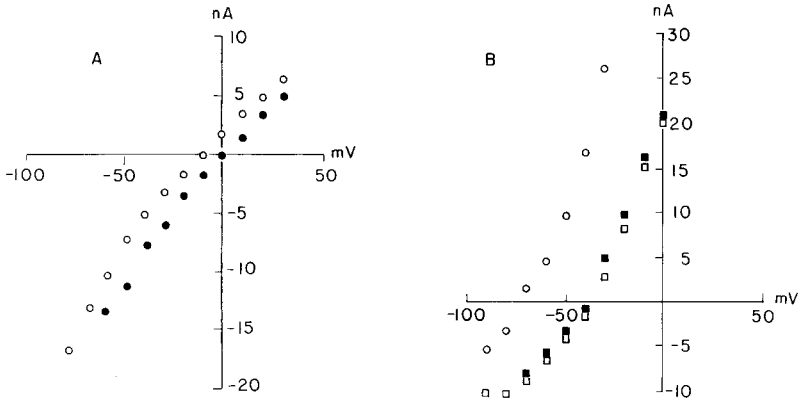

Fig. 9. Instantaneous current-voltage relationships for two cells bathed (*A*) in isotonic KCl (●) or RbCl (○) solutions or (*B*) in isotonic CsCl (□, ■) or NaCl (○) solutions; internal solution 1 (Table 1) in both cells. The two current-voltage relations in CsCl solution were obtained before and after the measurement in NaCl solution. Cell SK-16, $T=15\,°C$; Cell SK-22, $T=14\,°C$

the central ion, because the polarization vector is the response of the dielectric medium to the ion's field, and this field increases with q. The dependence of f on ion radius can be seen rigorously from a statistical mechanical treatment of the polarization vector that we will not present here. Qualitatively, however, one can see that the polarization vector (and hence f) would, at least near the ion surface, depend upon ion size; as the ion is made larger, the hydrogen bonded structure of water around the ion is disrupted, and this altered structure would be expressed in the average dipole moment per unit of volume, the polarization vector P.

Eq. (16) permits us to relate the coefficients in the power series expansion [Eq. (10)] to physical characteristics of the channel. A more detailed microscopic treatment of these coefficients uses a statistical mechanical approach mentioned earlier. The constant term in Eq. (10) is simply $B(X)$ from Eq. (16) evaluated for the reference ion whose size is specified by X_o. The quantity a_1 is given by

$$a_1 = \left(\frac{\partial B}{\partial X}\right)_{X=X_o} = \int_0^{\varepsilon} dq\, f(X_0, X_0, q) + \int_0^{x_o} dx \int_0^{\varepsilon} dq \left(\frac{\partial f(x, X, q)}{\partial X}\right)_{X=X_o}. \quad (17)$$

As can be seen, a_1 has two contributions: The first term in Eq. (17) depends on the difference in dipole moment at the reference ion surface when the ion is in its selectivity location as compared to water. This term would indicate the average dipole moment of the channel structure in contact with the ion as well as that contributed by the surrounding water molecules. The second term in Eq. (17) relates to the rate at which the dipole moment on each sphere around the ion changes as the ionic radius is altered. Such dipole moment changes occur by two mechanisms. The first is through alterations in the local electric field which is less intense around larger ions and thus produces less dipole arrangement; the second mechanism has to do with the altered structures of water necessary to accommodate a larger (or smaller) ion. Again because the channel protein structure is fixed and because this protein imposes constraints on the arrangements of water molecules through the various hydrogen bonding possibilities, this second term may be used as an indication of the "fluidity" of the channel and channel water structure as compared to free water. The smaller a pore, the more constraints placed on water so the larger this term would be. The higher order coefficients (a_2, a_3, etc.) can also be calculated and their physical significance elucidated, but this analysis rapidly becomes complex and will not be further pursued here.

Experimental Results

Instantaneous current-voltage relationships were obtained from an experimental protocol as illustrated in Fig. 3. They were measured either in isotonic KCl solution (external solution 2, Table 1) or in solutions where KCl had been replaced isosmotically by another salt (*see* Materials and Methods). Fig. 9*a* compare instantaneous current-voltage relationships measured in KCl (closed circles and RbCl (open circles) solutions. There is a 7.1 mV shift of V_o towards more negative potentials in RbCl solution. Fig. 9*b* shows results from another cell bathed in CsCl (squares) and NaCl (circles) solutions.

The current-voltage relation in NaCl solution was obtained between two runs in CsCl solution. Clear reversal potentials were measured in both solutions, but at much more negative potentials than under the conditions in Fig. 9*a*. Moreover, the channels rectify in opposite directions in Figs. 9*a* and *b* indicating partial block of the channels by Na and Cs ions. Another example is illustrated in Fig. 10 where isotonic KCl (squares) and guanidinium · HCl (dia-

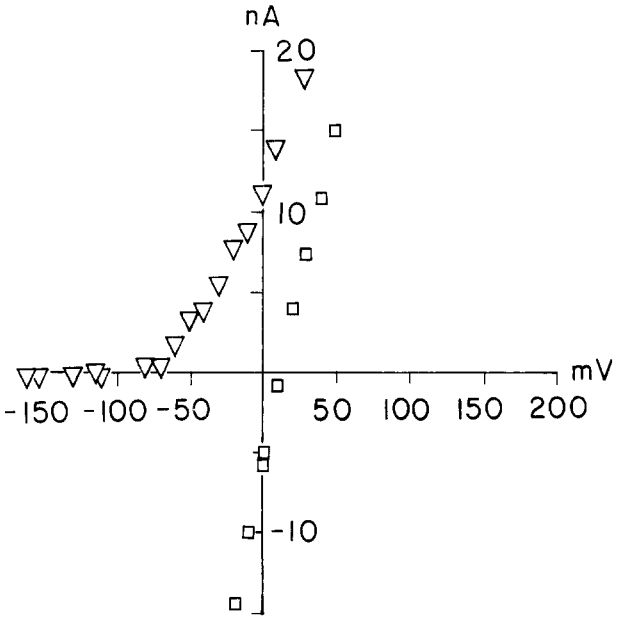

Fig. 10. Instantaneous current-voltage relationships of a cell bathed in isotonic KCl (□) or guanidinium · HCl (▽) solutions; internal solution 1 (Table 1). Cell SK-32, $T=16\,°C$

monds) solutions are compared. No clear reversal potential could be measured in the organic cation solution. Similarly, it was not possible to determine reversal potentials with other organic (hydroxylamine$^+$, hydrazine$^+$, methylamine$^+$) or divalent (Ba^{2+}, Sr^{2+}, Mg^{2+}) cations tested in these experiments. Although outward currents, carried by K^+ ions, were always prominent, no inward current tails could be detected at hyperpolarizing clamp steps up to -150 mV. This implies that potassium channels in snail neurones are virtually impermeable to small organic cations and divalent cations. Similar results were obtained by Hille (1973) in myelinated nerves of the frog.

In addition to the alkali metal cations K^+, Rb^+, Cs^+, Na^+, Li^+, delayed potassium channels are permeable to NH_4^+ and Tl^+ ions (*cf.* Hille, 1973). Table 3 summarizes all our results obtained from reversal potential measurements with permeable cations. Not only did we measure shifts of reversal potentials (V_k) by switching between an isotonic KCl solution and another isotonic monovalent cation solution, but we also compared poorly permeable cations (Na^+, Li^+, Cs^+, NH_4^+) directly with each other. The picture that emerged is self-consistent (Table 3).

Permeability ratios for the k^{th} ion compared to potassium were calculated from (*see* Theory)

$$P_k = \exp\left(\frac{-\Delta B_k}{RT}\right) \tag{8}$$

Table 3. Summary of ion selectivity experiments

k	i	V_k (mV) (±SE)	n	P_k
Rb	⟶ K	7.4±1.1	4	0.74
Cs	⟶ K	42.6±6.9	6	0.18
Li	⟶ K	59.6±5.8	5	0.09
Na	⟶ K	69.3±6.7	5	0.07
Na	⟶ Li	6.5±1.3	3	0.77
Li	⟶ Cs	16.6±1.8	2	0.52
Na	⟶ Cs	19.7±4.7	3	0.46
NH_4	⟶ K	48.5±4.6	4	0.15
Li	⟶ NH_4	18.4±8.9	2	0.47
Tl	⟶ K	−6.2±2.0	3	1.29

The first column k indicates the direction of the solution changes (from k to i); V_k is the change in reversal potential; n is the number of experiments; P_k is the permeability of the k^{th} compared to the i^{th} ion.

where

$$\Delta B_k = -FV_k + RT \ln\left(\frac{m_{0k}}{m_{1k}}\right). \tag{9}$$

ΔB_k is the selectivity barrier free energy that the k^{th} ion experiences relative to the potassium ion barrier, and M_{0k} and M_{1k} are ion activities of the k^{th} outside and potassium ion inside at 15 °C (Robinson & Stokes, 1959). In Fig. 11, ΔB_k is plotted as a function of reciprocal ion radii of alkali metal cations. The data points were obtained from average experimental values listed in Table 3. The theoretical curve has been calculated from expansion in Eq. (10) carried out to the cubic term and provides an excellent fit to the experimental data.

Permeability ratios calculated from the Goldman-Hodgkin-Katz equation (*see* Hille, 1973) were identical to those listed in Table 3.

Table 3 indicates the following selectivity sequence of the alkali metal cations passing through potassium channels in snail neurone membranes: $K^+ > Rb^+ > Cs^+ > Li^+ > Na^+$. Fig. 11 shows that this sequence is not a simple function of ion radii. Furthermore, this series does not conform to any of the eleven permutations for alkali metal cation selectivities suggested by Eisenman (1962; for reviews *see* Diamond & Wright, 1969).

In addition to alkali metal cations, Tl^+ and NH_4^+ were the only other cations tested in our experiments that were measurably permeable. In summary, delayed potassium channels in snail neurones are permeable to the cations Tl^+, K^+, Rb^+, Cs^+, NH_4^+, Li^+, Na^+ in the ratios 1.29:1.00:0.74:0.18:0.15:0.09:0.07. The relative permeabilities for Cs^+, Li^+ and Na^+ are somewhat higher than in frog myelinated nerve fibers (Hille, 1973) and frog skeletal muscle (Gay & Stanfield, 1978).

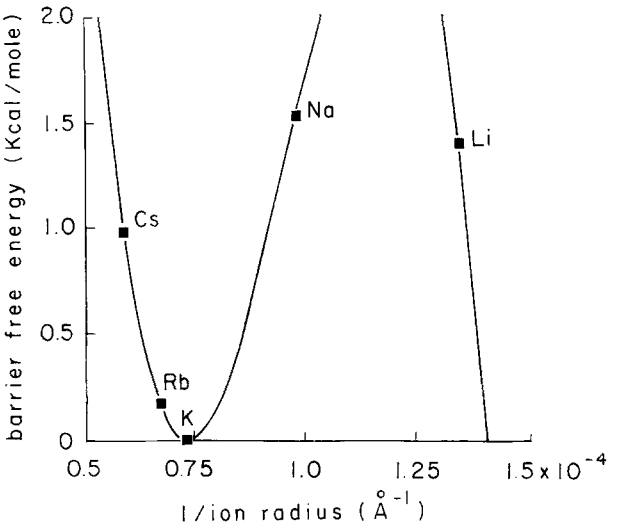

Fig. 11. Barrier-free energy for alkali metal cations in K channels plotted as function of reciprocal cation radii. Barrier-free energy (i.e., the difference between free energies of ions in the channel and in free solution) of various ions. Experimental points were obtained from data in Table 3; the curve fitted to the experimental points is interrupted between 1 and 1.3 $Å^{-1}$ and calculated from Eq. (10) with barrier heights plotted as differences from the potassium value, and with the expansion carried out around the potassium size (1/radius = 0.725 Å). Coefficients have values $a_1 = -0.573$, $a_2 = 40.89$ and $a_3 = -57.8$; ion sizes are measured in Å (Li: 1.351, Na: 0.98, K: 0.725, Rb: 0.671, Cs: 0.588) and barrier-free energy in kcal/mole

Table 4. Conductance ratios (g_{in}/g_{out}) estimated from inward and outward conductances at potentials negative and positive to V_o

External solution	g_{in}/g_{out} (±SE)	n
KCl	1.13±0.05	22
RbCl	1.59±0.09	8
CsCl	0.19±0.02	6
LiCl	0.31±0.04	9
NaCl	0.25±0.03	12
NH_4Cl	1.02±0.01	3
Tl acetate	1.30±0.11	4

From the ratio of the slope of outward conductance positive to V_o and that of inward conductance negative to V_o in experiments similar to those in Fig. 9 one obtains empirical rectification ratios for permeable cations. While outward conductance is predominantly or exclusively a K conductance, inward conductance is governed by the cation present in the external solution. From the results listed in Table 4 it is clear that very little rectification is seen with NH_4^+ or K^+ in the external medium. Inward conductance is slightly larger than outward conductance with external Tl^+ and Rb^+ ions. However, inward conductance is strongly reduced with Cs^+, Na^+ and Li^+, at negative potentials confirming the tendency of these ions to block potassium channels (Bezanilla & Armstrong, 1972; Hille, 1973).

Discussion

Our interpretation of the reversal potential measurements presented here depends strongly on our physical picture for ion permeation. Although we feel this picture is an entirely plausible one, it is subject to a number of uncertainties which we would like to emphasize. Chief among these are the possible importance of nonelectrostatic factors in determining barrier height, limitations in the hopping model, and the possibility that a single barrier is not rate limiting or that the rate-limiting barrier differs for different ions.

An example of a nonelectrostatic factor that might contribute to an ion's barrier height is the energy to displace water – that is, to create a cavity – at the selectivity site: the various ions require different sized cavities. The ions that pass through the potassium channels we have studied range in diameter from 0.74 to 1.7 Å as compared to a water molecule diameter of 1.38 Å (*see* Bockris & Reddy, 1973). Thus all of these ions approximately fit in the space vacated by a single water molecule, and the rearrangement of hydrogen bonds necessary to accommodate the variations in size should not give rise to energy differences that are as large and the electrostatic effects we have considered. For example, expanding the ion radius from K to Cs would amount to a size change of 0.3 Å, and a linear compression of a surrounding water hydrogen bond by this amount would require only about 0.1 kcal/mole (obtained from H-bond stretching frequency N = 160 cm^{-1}; Table 1.1 in Joesten and Schaad, 1974; *see also* H-bond potential function in, for example, Matsuoka, Clementi and Yoshimine, 1976). Bending and rotations of hydrogen bonds over small distances take very little energy (*see*, for example, Scheiner & Kern, 1977), so the displacements necessary to accommodate the various permeant ions would seem to require very little energy even in the restricted region of the pore. Similarly, chemical (rather than electrostatic) interactions of alkali metal cations with their surroundings should contribute little (Noyes, 1962). Nevertheless, these nonelectrostatic contributions to barrier height may not be completely negligible.

The theory we have used here is formally identical to the hopping model used to treat ionic diffusion in crystals (*see* Stevens & Tsien, 1979). Diffusion within the channel, however, is quite different from the situation in crystals where the ion moves a few ang-

stroms from one lattice site to another. Horn and Stevens (1980) have discussed implications of use of hopping models when individual "hops" are composite movements, and have considered some other potential difficulties with the approach we have adopted here.

The Born equation (11) used as the starting point for our theoretical development is rigorous, but is a macroscopic equation applied to a microscopic situation. Although we shall not present a more detailed theory here, a statistical mechanical treatment, similar to that used by Dogonadze and Kornyshev (1974), provides an appropriate microscopic interpretation for our equations. A difficulty with the theoretical development that cannot be easily surmounted, however, relates to the residence time of an ion at each location within the channel. We have carried out an electrostatic treatment to calculate the energy barrier, and this assumes that all relaxation times in the dielectric medium are rapid compared to the residence time of an ion in any location. Since these residence times are uncertain, so is the validity of this assumption. Those relaxation times which are longer than ion residence times could be ligitimately ignored in an approximate treatment, so the only difficulty would be relating quantities such as the dielectric constant that appeared in our equations to their microscopically defined counterparts.

We have assumed the existence of a single rate-limiting barrier that governs ion movement through the channel, but we must emphasize that we have no independent evidence for this assumption. Not only is it possible that two or more barriers may be comparable in magnitude, but also the position of barriers might depend on ion radius or other characteristics.

As we have stressed here, it is impossible to assess, at present, the adequacy of our physical picture or the magnitude of errors in our treatment. As physiological and structural information about this and other channels grows, we should gradually be able to evaluate the extent to which our picture is realistic, ultimately with detailed molecular dynamic studies. In the meantime, we view our conclusions as defining the selectivity phenomena we have studied in quantitative terms, and in providing a plausible physical basis for understanding them.

Data comparable to those presented here are available for the acetylcholine receptor channel of the frog neuromuscular junction (C.A. Lewis and C.F. Stevens, *unpublished observations*), and a comparison between the properties of the two channels is interesting. The acetylcholine receptor channel is very non-selective (Huang, Catterall & Ehrenstein, 1978) and, as would be expected for a not very selective channel, selectivity energy barrier height is a linear function of reciprocal ion radius; that is, only the linear term in Eq. (10) is required to describe this channel's selectivity. The potassium channel, on the other hand, is very selective and excludes all of the organic ions we have tested. The first coefficient in the expansion displayed in Eq. (10) is 0.34 kcal Å/mole for the acetylcholine activated channel and -0.57 kcal Å/mole for the potassium channel. This difference is understandable in terms of dimensions of the pore size which must be an aperture of diameter 6 or 7 Å for the acetylcholine-activated channel (*see* dimensions of permeant species studied by Huang et al., 1978) and perhaps only 3 or 4 Å for the potassium channel (Hille, 1973). Recall that the coefficient a_1 in Eq. (10) is composed of the two terms that appear in Eq. (17): the first term is the fixed dipole density at the surface of the reference ion and the second relates to the rate at which the dielectric properties of the medium around the ion change with ion diameter. For an unstructured pore interior, with few constraints placed on water by the protein walls of the pore, $\partial f/\partial x$ will contribute little because pore water will be about as fluid as bulk water; this is presumably the case for the "large" and quite unselective acetylcholine receptor channel were the fixed dipole term is responsible for selectivity. For the more constrained K channel, the first and higher derivatives of f become important and the sign of a_1 reverses, although the magnitude is roughly similar.

The selectivity barrier for the ammonium ion is smaller than would be anticipated on the basis of its size which is between K and Rb, but closer to Rb. Because this ion has tetrahedrally disposed hydrogens which form hydrogen bonds with surrounding molecules, the high permeability of ammonium is revealing. In water, the ammonium ion would normally form four hydrogen bonds, one with each hydrogen, and each with an energy on the order of 10 kilocalories per mole (Payzant, Cunningham & Kebarle, 1973). If within the pore ammonium ions formed fewer than four hydrogen bonds at the selectivity site, the energy barrier for them would be expected to be at least several kilocalories per mole higher than a comparably sized "nonreactive" ion. On the contrary, ammonium is more permeant than a comparably sized inert ion, so not only must it form about four hydrogen bonds, but one or more of these must be a little more stable than that normally formed with water. Because the energy of the ammonium ion within the pore is so close to that in bulk solution, it seems most likely that three of the four hydrogens formed bonds to water molecules within the channel, and that the fourth hydrogen bonds to some group on the polypeptide chain, perhaps a carbonyl oxygen,

incorporated within the walls of the channel. As carbonyl-ammonium hydrogen bonds are somewhat stronger than ammonium-water bonds (Scheiner & Kern, 1977), the selectivity of ammonium could be easily accounted for. If this picture is correct, hydrogen bonds on the channel walls must be available for the water molecules arranged at three corners of the ammonium ion tetrahedron.

Thallium, like ammonium, has a selectivity barrier lower than would be anticipated by its size which lies between that of K and Rb, but closer to Rb (Lee, 1977). This difference must be due to a more favorable interaction energy (as "partial covalency") with some constituent of the channel structure than with water (Krasne & Eisenman, 1973; Lee, 1977). Again, interactions with three water molecules and one more reactive group, such as a carbonyl oxygen, could give the barrier observed.

Because all of the permeant ions must experience an environment very similar to that in free solution, and because it seems that the ammonium ion probably interacts with three tetrahedrally arranged water molecules, the most plausible picture of ion permeation is one in which every ion passes through the narrowest part of the channel associated with a water structure much like that in free water. We would view the channel protein as providing hydrogen bonding sites that permit the permeating species to interact with a carbonyl oxygen and simultaneously with three tetrahedrally disposed waters which in turn had the possibility of hydrogen bonding to protein or other waters. Although speculative, this picture is a very specific one which we anticipate can be tested as more information about channel structure properties becomes available.

Financial support provided by U.S. Public Health Service grant NS-12961 (to Dr. Stevens) and Swiss National Science Foundation grant 3.374-0.78 (to Dr. Reuter) is gratefully acknowledged.

References

Adams, D.J., Gage, P.W. 1979. Ionic currents in response to membrane depolarization in an *Aplysia* neurone. *J. Physiol. (London)* **289**:115

Anderson, C.R., Stevens, C.F. 1973. Voltage clamp analysis of acetylcholine produced end-plate current fluctuations at frog neuromuscular junction. *J. Physiol. (London)* **235**:655

Armstrong, C.M. 1975. Ionic pores, gates, and gating currents. *Q. Rev. Biophys.* **7**:179

Begenisich, T., Stevens, C.F. 1975. How many conductance states do potassium channels have? *Biophys. J.* **15**:843

Bezanilla, F., Armstrong, C.M. 1972. Negative conductance caused by entry of sodium and cesium ions into the potassium channels of squid axons. *J. Gen. Physiol.* **60**:588

Bockris, J.O'M., Reddy, A.K.N. 1973. Modern Electrochemistry, Vol. 1. Plenum, New York

Born, M. 1920. Volumen und Hydratationswärme der Ionen. *Z. Phys.* **1**:45

Buckingham, A.D. 1957. A theory of ion-solvent interaction. *Faraday Soc. Disc.* **24**:151

Connor, J.A., Stevens, C.F. 1971*a*. Inward and delayed outward membrane currents in isolated neural somata under voltage clamp. *J. Physiol. (London)* **213**:1

Connor, J.A., Stevens, C.F. 1971*b*. Voltage clamp studies of a transient outward membrane current in gastropod neural somata. *J. Physiol. (London)* **213**:21

Conti, F., DeFelice, L.J., Wanke, E. 1975. Potassium and sodium ion current noise in the membrane of the squid giant axon. *J. Physiol. (London)* **248**:45

Diamond, J.M., Wright, E.M. 1969. Biological membranes: The physical basis of ion and nonelectrolyte selectivity. *Annu. Rev. Physiol.* **31**:581

Dogonadze, R.R., Kornyshev, A.A. 1974. Polar solvent structure in the theory of ionic solvation. *J. Chem. Soc. Faraday Trans. 2.* **70**:1121

Eisenman, G. 1963. Cation selective glass electrodes and their mode of operation. *Biophys. J.* **2** (suppl. 2):259

Fishman, H.M., Moore, L.E., Poussart, D.J.M. 1975. Potassium-ion conduction noise in squid axon membrane. *J. Membrane Biol.* **24**:305

Gay, L.A., Stanfield, P.R. 1978. The selectivity of the delayed potassium conductance of frog skeletal muscle fibers. *Pfluegers Arch.* **378**:177

Goldman, D.E. 1943. Potential impedance and rectification in membranes. *J. Gen. Physiol.* **27**:37

Heyer, C.B., Lux, H.D. 1976. Control of the delayed outward potassium currents in bursting pace-makers neurones of the snail. *Helix Pomatia. J. Physiol. (London)* **262**:349

Hille, B. 1973. Potassium channels in myelinated nerve. Selective permeability to small ions. *J. Gen. Physiol.* **61**:669

Hille, B. 1975. Ionic selectivity of Na and K channels of nerve membranes. *In:* Membranes—A Series of Advances, Vol. 3, Dynamic Properties of Lipid Bilayers & Biological Membranes. G. Eisenman, editor. p. 255. Marcel Dekker, Inc., New York

Hille, B. 1977. Ionic basis of resting and action potentials. *In:* Handbook of Physiology, The Nervous System I. E. Kandel, editor. p. 99. Williams & Wilkin, Baltimore

Hodgkin, A.L., Katz, B. 1949. The effect of sodium ions on the electrical activity of the giant axon of the squid. *J. Physiol. (London)* **108**:37

Horn, R., Stevens, C.F. 1980. Relation between structure and function of ion channels. *Comm. Mol. Cell. Biophys. (in press)*

Huang, L.M., Catterall, W.A., Ehrenstein, G. 1978. Selectivity of cations and nonelectrolytes for acetylcholine-activated channels in cultured muscle cells. *J. Gen. Physiol.* **71**:397

Joesten, M.D., Schaad, L.J. 1974. Hydrogen Bonding. Marcel Dekker, Inc., New York

Kostyuk, P.G., Krishtal, O.A. 1977. Separation of sodium and calcium currents in the somatic membrane of mollusc neurones. *J. Physiol. (London)* **270**:545

Kostyuk, P.G., Krishtal, O.A., Doroshenko, P.A. 1975. Outward currents in isolated snail neurones. II. Effect of TEA. *Comp. Biochem. Physiol.* **51C**:265

Kostyuk, P.G., Krishtal, O.A., Pidoplichko, U.T. 1975. Effects of internal fluoride and phosphate on membrane currents during intracellular dialysis of nerve cells. *Nature (London)* **257**:691

Krasne, S., Eisenman, G. 1973. The molecular basis of ion selectivity. *In:* Membranes-A Series of Advances, Vol. 2, G. Eisenman, editor. p. 179. Marcel Dekker, Inc., New York

Lee, A.G. 1977. The coordination chemistry of thallium (I). *Coord. Chem. Rev.* **8**:281

Lee, K.S., Akaike, N., Brown, A.M. 1978. Properties of internally

perfused, voltage clamped, isolated nerve cell bodies. *J. Gen. Physiol.* **71**:489

Matsuoka, O., Clementi, E., Yoshimine, M. 1976. Cl study of the water dimer potential surface. *J. Chem. Phys.* **64**:1351

Meech, R.W. 1978. Calcium-dependent potassium activation in nervous tissue. *Ann. Rev. Biophys. Bioeng.* **7**:1

Meech, R.W., Standen, N.B. 1975. Potassium activation in *Helix aspersa* neurones under voltage clamp: A component mediated by calcium influx. *J. Physiol. (London)* **249**:211

Meves, H. 1968. The ionic requirements for the production of action potentials in *Helix pomatia* neurones. *Pfluegers Arch.* **304**:215

Neher, E. 1971. Two fast transient current components during voltage clamp on snail neurones. *J. Gen. Physiol.* **58**:36

Neher, E., Lux, H.D. 1973. Rapid changes of potassium concentration at the outer surface of exposed neurones during membrane current flow. *J. Gen. Physiol.* **61**:385

Neher, E., Stevens, C.F. 1977. Conductance fluctuations and ionic pores in membranes. *Annu. Rev. Biophys. Bioeng.* **6**:345

Noyes, R.M. 1962. Thermodynamics of ion hydration as a measure of effective dielectric properties of water. *J. Am. Chem. Soc.* **84**:513

Partridge, L.D., Stevens, C.F. 1976. A mechanism for spike frequency adaptation. *J. Physiol. (London)* **256**:315

Payzant, J.D., Cunningham, A.J., Kebarle, P. 1973. Gas phase solvation of the ammonium ion by NH_3 and H_2O and stabilities of mixed clusters $NH_a(NH_3)_n(H_2O)_w$. *Can. J. Chem.* **51**:3242

Robinson, R.A., Stokes, R.H. 1959. Electrolyte Solutions. Butterworths, London

Scheiner, S., Kern, C.W. 1977. Theoretical studies of environmental effects on protein conformation. 1. Flexibility of the peptide bond. *J. Am. Chem. Soc.* **99**:7042

Siebenga, E., Meyer, A.W.A., Verveen, A.A. 1973. Membrane shot-noise in electrically depolarized nodes of *Ranvier. Pfluegers Arch.* **341**:87

Sigworth, F.J. 1979. Analysis of nonstationary sodium current fluctuations in frog myelinated nerve. Ph.D. Thesis, Yale University, New Haven, Connecticut

Stevens, C.F. 1972. Inferences about membrane properties from electrical noise measurements. *Biophys. J.* **12**:1028

Stevens, C.F., Tsien, R.W. 1979. Membrane Transport Processes. Vol. 3. Ion Permeation Through Membrane Channels. Raven Press, New York

Thompson, S.H. 1977. Three pharmacologically distinct potassium channels in molluscan neurones. *J. Physiol. (London)* **265**:465

Wolbarsht, M.L., MacNichol, E.F., Wagner, H.G. 1960. Glass insulated platinum electrode. *Science* **132**:1309

Received 26 February 1980